The Impact of Antenna Directivity and Channel Bandwidth on the Power Spectral Density of Wideband and UWB MISO Channels

Ana-Maria Pistea
Communications
TUCN
Cluj Napoca, Romania
ampistea@gmail.com

Tudor Palade
Communications
TUCN
Cluj Napoca, Romania
palade@com.utcluj.ro

Ancuta Moldovan
Communications
TUCN
Cluj Napoca, Romania
Ancuta.Moldovan@com.utcluj.ro

Hamidreza Saligheh Rad
Department of Radiology
UPENN
Philadelphia, USA
hamid.saligheh@gmail.com

Abstract—**The combination of MIMO with wideband (WB) and ultra-wideband (UWB) systems imply many new effects, which make the conventional channel models developed for narrowband transmissions to be inadequate for communications with large bandwidth. In this paper we use the Fourier analysis of the cross-correlation functions (CCF)s between the space-time-frequency (STF) transfer functions of two sub-channels of an outdoor WB/UWB MIMO wireless channel to derive the power spectral density (PSD) in a stationary scenario. The assumptions of the stationary scenario transform the MIMO channel into a Multiple-In Single-Out (MISO) channel and the PSD is determined when the channel bandwidth is wide or ultra-wide. The Fourier analysis of the CCF reveals the fact that the PSD deviates from the U-shaped function, i.e., Clarke/Jake's model to a great extent. This deviation is strongly influenced by the antenna directivity and the channel bandwidth. One major phenomenon which become stronger when the bandwidth increases is the frequency selectivity which is obviously larger in case of UWB channels than in case of WB channels. This characteristic makes possible the recognition of the type of the channel for its bandwidth from its PSD only.**

Keywords-WB; UWB; MIMO; wireless channel; PSD.

I. INTRODUCTION

The design of high performance wideband (WB) and ultra-wideband (UWB) multiple-input multiple-output (MIMO) wireless systems, requires accurate prediction of the impact of random multipath propagation and reliable MIMO channel models which take into account the impact of the direction-of-departure (DOD), direction-of arrival (DOA), time of arrival (TOA) and the system bandwidth [2], [3].

The cross-correlation function (CCF) of two sub-channels of an outdoor WB/UWB MIMO wireless channel [1] is used to determine the Power Spectral Density (PSD) of WB and UWB channels in a stationary scenario. The mathematical set-up of the stationary scenario transforms the MIMO channel into a Multiple-In Single-Out (MISO) channel. We analyzed a stationary MISO channel as a special case of MIMO channel. The PSD is derived for outdoor channels, when omnidirectional and directional antennas are employed at the mobile station (MS), in a 2D non-isotropic propagation environment. The CCF expression is based on the space-time-frequency (STF)

channel transfer functions (CTF) which is represented by a sum of cluster waves over a number of dominant paths . We derive the PSD using the Fourier analysis of the CCF of MIMO channels. In the literature are other works which present results obtained by using the classical approach that applies the direct Fourier relation between the correlation and the PSD [2], [3]. The majority of these models employ a specific geometry for the scatterers around the MS [4], [5], [6]. Based on this approach each model is just capable to predict the behavior of that particular propagation scenario [8]. Moreover, they are not able to investigate the spatial, the temporal, and the frequency aspects of the wireless channel in one single model. Alternatively in this paper, we do not assume a certain geometry to describe the relative distribution of scatterers in the space. We establish a mathematical relation between the random time-delay and the random channel-gain associated with each scattered waveform within each cluster and use appropriate pdfs for the parameters such as the time-delay, the DOA and the DOD. As a result the derived PSD is based on a non-geometry approach, describing the non-isotropic propagation by using appropriate pdfs for the parameters such as the time-delay, DOA and DOD. The expression of the PSD is the Fourier transform of a linear series expansion of a number of Bessel functions of the first kind. The coefficients of the expansion of the PSD are described by three categories of Fourier series coefficients (FSC): a) linear convolution of the FSC of the antenna pattern, b) the FSC of the azimuth angular spread and c) the Fourier series expansion (FSE) of the pdfs describing the non-isotropic environment.

This paper is organized as follows: the 2D channel model is described in Section 2. In Section 3, the mathematical model of the CCF it is presented. In Section 4, the PSD equation is derived and it is numerically evaluated under different circumstances. Conclusions are presented in Section 5.

II. TWO DIMENSIONAL WB/UWB MIMO MODEL DESCRIPTION

In this section, we describe the propagation scenario and the notations used throughout this paper in which superscripts B

and M indicate the variables at BS and MS sides, respectively. We also emphasize the differences which exist between WB and UWB channel models and how these differences are included in our model.

We consider a moving MS with a constant speed vector $V\left(\frac{m}{sec}\right)$ and a fixed BS in a 2D non-isotropic propagation environment where the multipath components arrive in clusters. The resulted CTF determined by the pth transmitting antenna element at BS side, the propagation environment and the mth receiving antenna element at MS side is the summation of the dominant I paths and L clusters. CTF expression includes the following elements:

E1) The antenna propagation patterns (APP)s of the pth and mth antenna of the BS and MS array, $G_p^B\left(\Theta_{il},\omega\right)$, $G_m^M\left(\Theta_{il},\omega\right)$ give the response of the antenna in terms of the propagation directions and frequency. These functions implicitly include the effect of mutual coupling caused by the neighboring antenna elements. Are all periodic functions of Θ_{il}^B- DOD of the ith dominant path in the lth cluster from the BS; and Θ^M- DOA of the ith dominant path in the lth cluster to the MS, with the same period of 2π. Therefore, we represent them by their FSEs as follows:

$$G\left(\Theta;\omega\right) = \sum_{k=-\infty}^{\infty} \mathcal{G}_k e^{jk\Theta}, \, \mathcal{G}_k = \frac{1}{2\pi}\int_{-\pi}^{\pi} G\left(\Theta;\omega\right)e^{-jk\Theta}d\Theta \tag{1}$$

For the WB channel, it is assumed that the response of the antenna does not change significantly over the bandwidth since the relative bandwidth is a small fraction of the central frequency. UWB antenna patterns are different at different frequencies and this characteristic should be considered in our model. In fact this is the main difference between channel models for WB signals and channel models for UWB signals. Thus, depending on the signal bandwidth, we will have two approaches for APP calculation:

a) for WB signals, APP is calculated depending on the central frequency, ω;

b) for UWB signals, we calculate the APP depending on the central freuency and by integrating $G\left(\Theta,\omega\right)$ across all the frequencies of the transmitted signal.

Table I presents the APPs of two WB/UWB antennas. The helical (directional) and rectangular (omnidirectional) antennas are often used for antenna arrays and WB/UWB applications [7]. The Fourier coefficients of omnidirectional antenna can be simply given by $\mathcal{G}_k = \delta_k$, where δ_k is the unit impulse [8]. In this case, the corresponding coefficients, $\mathcal{G}_k$, vanish from the expression of the CCF and the channel bandwidth influence can not be determined. Since in the case of WB and UWB channels, the bandwidth has a great impact on the channel statistics, it's necessary to replace $\mathcal{G}_k = \delta_k$ with the $\mathcal{G}_k$ of rectangular antennas which allow us to see the influence of the channel bandwidth.

Table I: 2D Antenna propagation patterns

Antenna Type		APP, $G_W\left(\Theta,\omega\right), \forall \Theta \in [-\pi,\pi)$
Helical antenna	WB	$j\, G_0 \cdot \frac{\omega}{2c}\cdot h \cdot sin\Theta$
	UWB	$\frac{1}{(f_H-f_L)}\int_{f_L}^{f_H} j\, G_0 \cdot \frac{\omega}{2c}\cdot h \cdot sin\Theta d\omega$
Rectangular antenna	WB	$j\, G_0 \frac{sin\left(\frac{\omega}{2c}\cdot h \cdot sin\Theta\right)}{\frac{\omega}{2c}\cdot h \cdot sin\Theta}$
	UWB	$\frac{1}{(f_H-f_L)}\int_{f_L}^{f_H} j\, G_0 \frac{sin\left(\frac{\omega}{2c}\cdot h \cdot sin\Theta\right)}{\frac{\omega}{2c}\cdot h \cdot sin\Theta}d\omega$

ω is the channel center frequency, f_H, f_L are the upper and lower frequencies of the UWB channel bandwidth, the parameter h is proportional with the size of the antenna and G_0 is the real and positive constant antenna gain that varies for each antenna.

Figure 1 shows the FSCs of the propagation patterns for WB and UWB antennas when $h = \frac{c}{2f}$. In the case of WB channels the antenna size is considered at the frequency $f = \frac{\omega}{2\pi} = 2.4$ GHz and for UWB channels we calculated the antenna size at $f = \frac{\omega}{2\pi} = 10.6$ GHz. We observe that for these antennas, the value of $\mathcal{G}_k$ is considerable only for a limited number of coefficients.

(a) WB Helical antenna

(b) WB Rectangular antenna

(c) UWB Helical antenna

(d) UWB Rectangular antenna
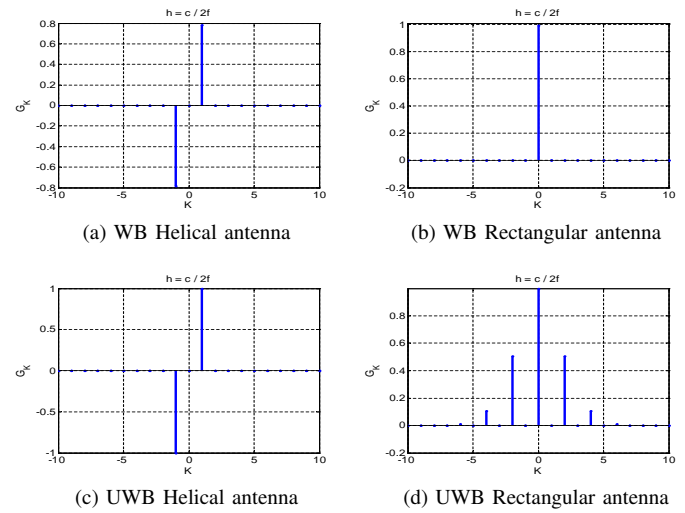
Figure 1: Normalized Fourier Series Coefficients for WB-APPs and UWB-APPs, $\frac{\mathcal{G}_k}{max_l|\mathcal{G}_l|}$, with antenna size: $h = \frac{c}{2f}$.

E2) The PDF of the propagation directions, $f^B\left(\Theta^B\right)$ and $f^M\left(\Theta^M\right)$, characterizes the non-isotropic environment. One candidate for the pdf of the non-isotropic AAS called Laplace distribution is presented in [9]. Another distribution which characterizes the non-isotropic environment is the von-Mises pdf[5]. Since these pdfs are periodic functions with period 2π, in Table II we represent them by the Fourier series coefficients (FSCs):

$$f_\Theta\left(\Theta\right) = \sum_{k=-\infty}^{+\infty} \mathcal{F}_k e^{jk\Theta}, \quad \mathcal{F}_k = \frac{1}{2\pi}\int_{-\pi}^{\pi} f_\Theta\left(\Theta\right)e^{-jk\Theta} \tag{2}$$

The von-Mises pdf is strongly influenced by the parameter n which determine the order of the channel non-isotropy. In other

words n controls the width of DOA of scatter components. The values of n can be chosen between $n \in [0, \infty)$. When $n = 0$, $f_{\Theta M}(\Theta) = \frac{1}{2\pi}$ this is equivalent with isotropic scattering.

Table II: Non-isotropic AAS and corresponding Fourier series coefficients

PDF, $f_\Theta(\Theta)$, $\forall \Theta \in [-\pi, \pi)$, $\mathcal{F}_k$	
Laplace	$f_\Theta(\Theta) = \dfrac{e^{\left| \frac{-\sqrt{2}\Theta}{\sigma} \right|}}{\sqrt{2}\sigma}$
	$\mathcal{F}_k = \dfrac{e^{-\frac{\pi(\sqrt{2}+jk\sigma)}{\sigma}} \left(e^{\frac{2\sqrt{2}\pi}{\sigma}} - e^{j2k\pi} \right)}{2\pi \left(-2 + j\sqrt{2}k\sigma \right)}$
von-Mises	$f_\Theta(\Theta) = \dfrac{e^{|n*cos(\Theta-\mu)|}}{2\pi J_0(n)}$
	$\mathcal{F}_k = \dfrac{J_k(n)}{J_0(n)}$

When $n \to \infty$, $f_{\Theta M}(\Theta) = \delta(\Theta - \mu)$, the propagation environment is considered extreme non-isotropic scattering concentrated at $\Theta = \mu$, where $\mu \in [-\pi, \pi)$ is the mean DOA at the MS. For large n, say $n \geqslant 3$ we have a typical non-isotropic environment [10]. When FSCs are determined the parameter n appears as the argument of the Bessel functions, where $J_k(\cdot)$ is the modified Bessel function of the first kind and $J_0(\cdot)$ is the zero-order modified Bessel function.

Figure 2 compares the FSCs of Laplace and von Mises pdf (at the MS). For the von-Mises distribution, FSCs are presented when the propagation environment has two different orders of non-isotropy.
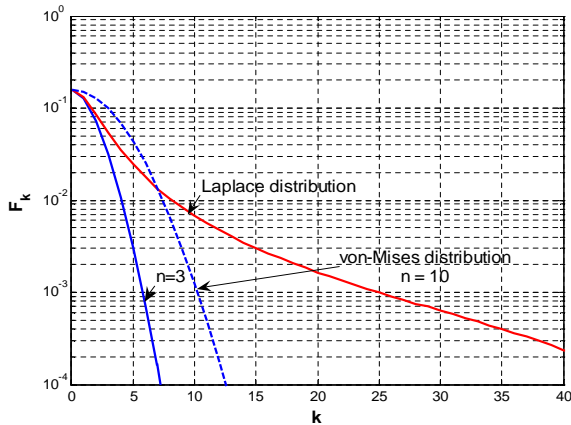
Figure 2: Fourier series coefficients for different AAS pdfs, to approximate Laplace and von-Mises distributions (with different orders of non-isotropy $n = 3, 10$) determined to have a good match to the real pdf for the non-isotropic propagation

Comparing the distributions in Figure 2, we see that the necessary number of FSCs for the Laplace pdf is larger than the necessary number of FSCs for the von-Mises pdf. One can observe that the required number of the FSCs increases when the non-isotropic characteristic of the propagation environment becomes more pronounced.

E3) The most significant effect for WB/UWB channels is the different attenuation that the sub-bands undergo. This phenomenon is known as frequency selectivity.

In our model the frequency selectivity of the radio channel is characterized by the term $\left(\frac{\omega_{bw}}{\omega} \right)^\eta$, where ω_{bw} is the signal bandwidth $\omega_{bw} = \omega_H - \omega_L$, ω_L, and ω_H are the lower and the upper frequencies, ω is the central frequency. η depends on the geometric configuration of the objects which produce signal's diffraction. Depending on the geometric configuration of the objects, η can take the values: -1 (diffraction by corner or tip), 0.5 (diffraction by axial cylinder face), 1(diffraction by broadside of a cylinder).

E4) The ith path (of the lth cluster) propagation delay, $\tau_{pm,il}$ is decomposed into three components [8]: one component which represents the delay depending on the distances between BS and MS, and another two components which vary as a function of the local coordinates of BS and MS:

$$\tau_{pm,il} = \tau_{il} - \left(\tau_{p,il}^B + \tau_{m,il}^M \right) \tag{3}$$

$$\tau_{p,il}^B \triangleq \frac{a_p^B \Theta_{il}^B}{c}; \quad \tau_{m,il}^M \triangleq \frac{a_m^M \Theta_{il}^M}{c} \tag{4}$$

where $\tau_{i,l}$ is the delay between local coordinates O^B or O^M, $\tau_{p,il}^B$, $\tau_{m,il}^M$ represents the propagation delays from antenna a_p^B to a_m^M located in their corresponding coordinates O^B or O^M. T_l is the cluster arrival rate and is considered to be constant in time. Θ_{il}^B is the unity vector pointing to the DOD of the $i \times l$th dominant path from the BS and Θ_{il}^M is the unity vector pointing to the DOA of the $i \times l$th dominant path to the MS.

E5) When modeling narrowband channels, it was adequate to define the path gain depending on the path time-delay [8]. This is not sufficient for WB/UWB MIMO channels where the frequency selectivity phenomenon influences the gain of the channel. In the ray based propagation models which can be applied to signals transmitted at high frequencies range, like WB and UWB signals, can be assumed that one propagation path has DOA and TOA that does not depend on frequency, but has a frequency dependent complex path gain. In our model the multipath gain is expressed as the extension of Friis' Transmission Formula [11]: $g_{mp,il} = \frac{1}{2\omega \tau_{il}}$.

E6) Assuming plane wave propagation the path phase shift, $\psi_{mp,il}$, can be accurately approximated by ψ_{il}. This is absolutely a function of the distance between the BS and the MS and on the signal frequency, and not a function of the position of different antenna elements in their coordinates [8]. The term $\psi_{il} = \phi_{il} - \omega(\tau_{il} + T_l)$ characterizes the phase shift depending only on the distance between the BS and the MS and the signal frequency, and not a function of the position of different antenna elements in their coordinates [12]. $\psi_{il} \sim U[-\pi, \pi)$ and illustrates the phase contribution of surrounding scatterers. We express the path phase shift in the form $e^{j(\phi_{il} - \omega(\tau_{il} + T_l))}$.

When putting together the elements described in E1÷E6, the CTF has the following expression:

$$h_{pm}(t, \omega) = \left(\frac{\omega_{bw}}{\omega} \right)^\eta \sum_{l=1}^{L} \sum_{i=1}^{I} G_p^B \left(\Theta_{il}^B; \omega \right) G_m^M \left(\Theta_{il}^M; \omega \right) \times$$

$$\times g_{pm,il} e^{j(\phi_{il} - \omega(\tau_{il} + T_l) - \overline{\omega_{il}}t - \omega\tau_{il} - \omega T_l)} \tag{5}$$

In the resulted CTF each l cluster, and implicitly each i wave, is associated with a path attenuation gain, $g_{pm,il}$, a path phase shift, ψ_{il}, a time-varying delay, $\tau_{pm,il}$. The Doppler shift of the ith received wave, within the lth cluster, is represented by $\overline{\omega_{il}} = \frac{\omega}{c} V^T \Theta_{il}^M$ where V and c are the MS velocity vector and the speed of light, respectively.

III. TWO DIMENSIONAL CROSS-CORRELATION FUNCTION OF WB/UWB MIMO CHANNELS

The CCF expression of the TFs, $h_{pm}(t_1, \omega_1)$ and $h_{qn}(t_2, \omega_2)$, of two arbitrary sub-channels of a MIMO channel is the result of the following definition:

$$R_{pm,qn}(t_1, t_2, \omega_1, \omega_2) \triangleq E\left[h_{pm}(t_1, \omega_1) h_{qn}^*(t_2, \omega_2)\right] \quad (6)$$

In the CCF expression are three dimensions: space, two pairs of antenna elements (p, m, q, n), time (t_1, t_2), and central frequencies (ω_1, ω_2). According to these three dimensions, we call it STF-CCF. The expectation operation is performed over all introduced random variables. In the presence of enough number of multi-paths by invoking the central limit theorem the TF can be considered a Gaussian random process. Therefore, the above second-order statistics fully characterize statistical behavior of the channel.

By replacing (5) in (6), regrouping dependent and independent random variables, using the elements described in E1-E6 and the results presented in [1] the CCF results in the following expression:

$$R_{pm,qn} = (t_1, t_2, \omega_1, \omega_2) \frac{(\omega_{bw1}\omega_{bw2})^\eta}{(\omega_1\omega_2)^\eta (4\omega_1\omega_2)}$$
$$\times \Phi_\tau (j(\omega_1 - \omega_2)) \Phi_\tau^{-(1)}(j(\omega_1 - \omega_2)) \Phi_T(j(\omega_2 - \omega_1))$$
$$\times \left\{ \mathcal{W}\left(d_{p,q}^B, \mathcal{G}_{p,k}^B(\omega_1) \otimes \mathcal{G}_{q,-k}^{B*}(\omega_2) \otimes \mathcal{F}_k^B\right) \right.$$
$$\left. \times \mathcal{W}\left(d_{m,n}^M, \mathcal{G}_{m,k}^M(\omega_1) \otimes \mathcal{G}_{n,-k}^{M*}(\omega_2) \otimes \mathcal{F}_k^M\right) \right\} \quad (7)$$

where

$$\mathcal{W}(d, \mathcal{H}_k) \triangleq 2\pi \sum_{k=-\infty}^{\infty} j^k e^{jk\angle d} \mathcal{H}_k(\omega) J_k\left(\frac{|d|}{c}\right) \quad (8)$$

$$d_p^B \triangleq \omega_1 d_p^B, \quad d_q^B \triangleq \omega_2 d_q^B, \quad d_{p,q}^B \triangleq \omega_1 a_p^B - \omega_2 a_q^B$$
$$d_m^M \triangleq \omega_1 \left(a_m^M - t_1 V\right), \quad d_n^M \triangleq \omega_2 \left(a_n^M - t_2 V\right)$$
$$d_{m,n}^M \triangleq (\omega_2 t_2 - \omega_1 t_1) V + \left(\omega_1 a_m^M - \omega_2 a_n^M\right)$$

$\mathcal{G}_{(\cdot,k)}^{(\cdot)}$ and $\mathcal{F}_k^{(\cdot)}$ are the kth FSCs of the APP and the AAS in the corresponding coordinates, respectively. $J_k(u) \triangleq \frac{j^{-k}}{\pi} \int_0^\pi e^{j(k\xi + u\cos\xi)} d\xi$ is the kth-order Bessel function, $\otimes$ and $|\cdot|$ denotes linear convolution and the Euclidian norm, respectively.

The norm of the separation vectors $d_{p,q}^B$, $d_{m,n}^M$ represent shifted distances between between $\omega_1 a_p^B$ and $\omega_2 a_q^B$ at the BS, and between $\omega_1\left(a_m^M - t_1 V\right)$ and $\omega_2\left(a_n^M - t_2 V\right)$ at the MS respectively. Large distances often result in less STF correlation as the Bessel functions asymptotically decrease. Parameters $d_{(\cdot,\cdot)}^{(\cdot)}$ contain space, time, and frequency separations between $h_{pm}(t_1, \omega_1)$ and $h_{qn}(t_2, \omega_2)$.

IV. TWO-DIMENSIONAL POWER SPECTRAL DENSITY OF 2D WB AND UWB MISO CHANNELS

We analyze the CCF derived in equation (7) in the frequency domain in order to see the temporal variations of the wireless channel. This analysis corresponds to the stationary scenario when $\omega_1 = \omega_2 = \omega$ and $m = n = 1$. This is the case MISO system. From $\angle d_{1,1}^M = \angle V + \angle (t_2 - t_1)$ we get:

$$R_{p1,q1}(t_1, t_2, \omega, \omega) = \pi \frac{\omega_{bw}^{2\eta}}{2\omega^{2\eta+2}} \mathcal{W}\left(d_{p,q}^B, \mathcal{H}_k^B\right)$$
$$\times \sum_{k=-\infty}^{\infty} j^k e^{jk\angle V}\left(\mathcal{G}_{1,k}^M(\omega_1) \otimes \mathcal{G}_{1,-k}^{M*}(\omega_2) \otimes \mathcal{F}_k^M\right)$$
$$\times J_k\left(\frac{\omega(t_2 - t_1)|V|}{c}\right) \quad (9)$$

Using the Fourier transform of $J_k(u)$, the Fourier transform of the CCF derived for stationary case versus the time-difference index, $\Delta t \triangleq t_2 - t_1$ results in the following equation:

$$R_{p1,q1}(\Lambda, \omega) \triangleq \int_{-\infty}^{\infty} e^{-j\Lambda\Delta t} R_{1p,1q}(t_1, t_2, \omega, \omega) d\Delta t$$
$$= \frac{\omega_{bw}^{2\eta}}{2\omega^{2\eta+2}} \mathcal{W}\left(d_{q,p}^M, \mathcal{H}_k^B\right) \frac{\pi c}{|V|}$$
$$\times \sum_{k=-\infty}^{\infty} \left(e^{jk\angle V} \mathcal{G}_{1,k}^M(\omega) \otimes \mathcal{G}_{1,-k}^{M*}(\omega) \otimes \mathcal{F}_k^M\right) \frac{T_k\left(\frac{c\Lambda}{|V|\omega}\right)}{\sqrt{1 - \left(\frac{c\Lambda}{|V|\omega}\right)^2}} \quad (10)$$

where $\mathcal{H}_k^B \triangleq \mathcal{G}_{p,k}^B(\omega) \otimes \mathcal{G}_{q,-k}^{B*}(\omega) \otimes \mathcal{F}_k^B$ and Λ is a frequency variable in the interval $\frac{\omega}{c}|V| < \Lambda < \frac{\omega}{c}|V|$. Note that $R_{p1,q1}(\Lambda, \omega) = 0$ for all $|\Lambda| \geqslant \frac{\omega}{c}|V|$. The Chebyshev polynomials form a complete orthogonal set on the interval $-1 \leqslant u < 1$, with respect to the weighting function $\frac{1}{\sqrt{1-u^2}}$. Therefore, any bandlimited CCF (on the interval $-\frac{\omega}{c}|V| \leqslant \Lambda \leqslant \frac{\omega}{c}|V|$) can be expanded in terms of Chebyshev polynomials as shown in the above expression.

In the following, $R^M(\Lambda)$ is the last term in 10, and represents the impact of the non-isotropic environment, the APP, and the direction of the MS speed:

$$R^M(\Lambda) \triangleq \sum_{k=-\infty}^{\infty} e^{jk\angle V}\left(\mathcal{G}_{1,k}^M(\omega) \otimes \mathcal{G}_{1,-k}^{M*}(\omega) \otimes \mathcal{F}_k^M\right)$$
$$\times \frac{T_k\left(\frac{c\Lambda}{|V|\omega}\right)}{\sqrt{1 - \left(\frac{c\Lambda}{|V|\omega}\right)^2}} \quad (11)$$

The term $R^M(\Lambda)$, is a PSD that represents the channel variations caused around or by the MS.

In Figures 3 and 4, this PSD is depicted for WB signals depending on the central frequency $f = 2.5\,GHz$ and for UWB for the bandwidth $3.1 \div 10.6\,GHz$, depending on the following elements:

i) the non-isotropic propagation environment around the MS is represented by Laplace and von-Mises distributions,

ii) the WB and UWB antennas employed at the MS side are represented by the helical and rectangular APPs,

iii) the direction of the MS speed is on the positive x-axis or the positive y-axis direction.

Analyzing the presented results we observe that three of the most important parameters which influences the PSD shape are APPs, the pdf of the propagation directions, the mobile speed direction and the channel bandwidth. The following observations can be formulated:

- For both WB and UWB channels, the maximum Doppler shift is $\frac{\omega}{c}|V|$ (i.e., $R^M(\Lambda) = 0$, if $|\Lambda| \geqslant \frac{\omega}{c}|V|$).
- These results are consistent with the results proposed in [8], [13], [14]. In [8] it is presented the PSD of a narrowband channel in non-isotropic 2D propagation. The results presented in this work are similar to the PSD shape we obtained for WB channels. Between our results and the results presented in [8] there are similarities regarding the U-shape of the PSD but there are also differences determined by parameters characteristic to wideband channels like frequency selectivity, higher central frequency and APPs typically used for these types of channels. Comparing the PSD obtained for WB channels with those obtain for UWB channels, and even with those obtained for narrowband channels in [8] we can conclude that the channel bandwidth has a great influence on the PSD shape. When the bandwidth increases the channel frequency selectivity also increases and larger variations can be observed over the PSD anvelope. The increased frequency selectivity is obviously larger in case of UWB channels than in case of WB channels. This feature offers the possibility to recognize the type of the channel for its bandwidth from its PSD only.
- It is clear that the majority of incoming/outgoing waves do travel in nearly horizontal directions and when the APP is directed along the vehicle motion the PSD has an asymmetrical shape. This is what it can be observed in our results: in Figure 3 when MS moves in the positive direction of the x-axis the PSD is larger at positive Λ than at negative Λ. This phenomenon is the consequence of the interaction between the beam of the antenna pattern, the direction of the MS speed, and the distribution of the propagation directions around the MS. This asymmetry of the PSD, is also determined by the Doppler spectrum which concentrates towards positive frequency axis.
- In Figure 4.4 all the PSD curves are symmetrical around the axis $\Lambda = 0$, because the pdf of the path directions and the APPs are symmetrical around $\Theta^M = 0$, and are perpendicular toward the speed direction.
- Generally speaking the PSD resulted for WB channels is less fluctuating than the PSD resulted for UWB channels. These fluctuations in the shape of the PSD of WB/UWB channels is the consequence of the frequency selectivity which increases with the signal frequency and signal bandwidth.
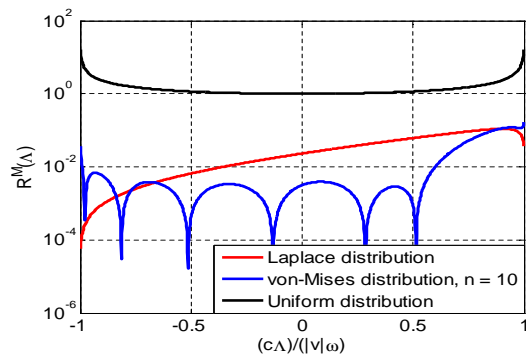
(a) Helical antenna
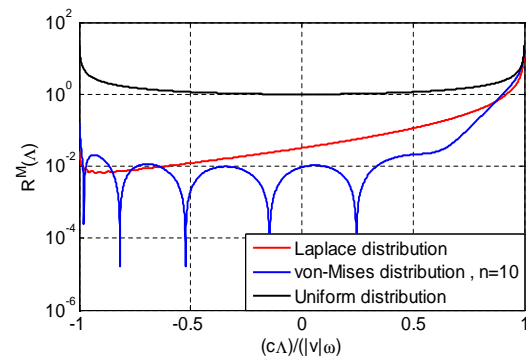
(b) Rectangular antenna
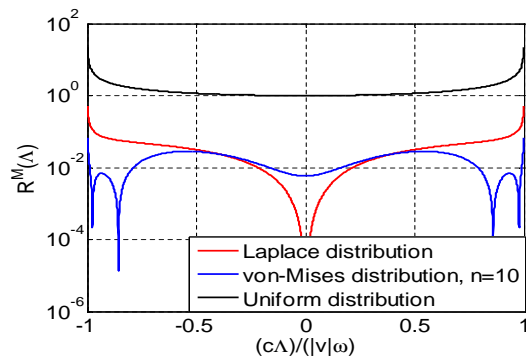
(c) Helical antenna
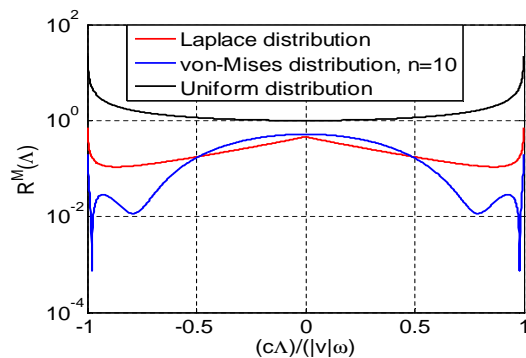
(d) Rectangular antenna

Figure 3: PSD of WB channels, MS moves in the positive direction of the x-axis (a,b) and y-axis (c,d), two antenna types employed at the MS, non-isotropic propagation (Laplacian or von-Mises distributed) and isotropic environment (uniformly distributed).

(a) Helical antenna

(b) Rectangular antenna

(c) Helical antenna

(d) Rectangular antenna
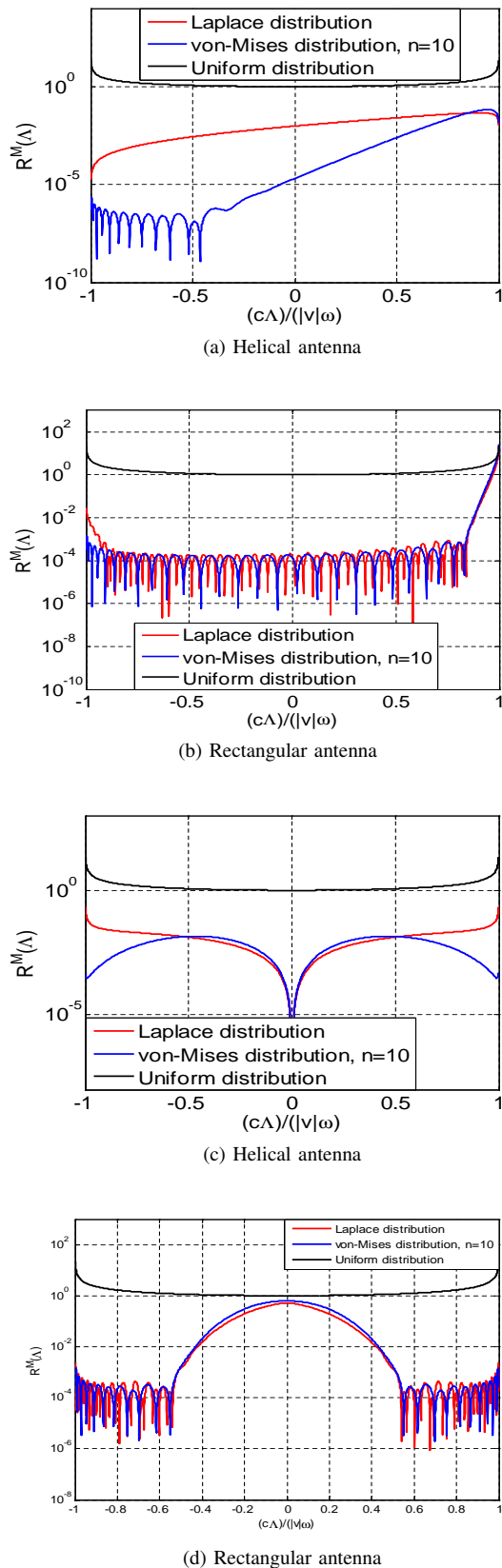
Figure 4: PSD of UWB channels, MS moves in the positive direction of the x-axis (a,b) and y-axis (c,d), two antenna types employed at the MS, non-isotropic propagation (Laplacian or von-Mises distributed) and isotropic environment (uniformly distributed) .

V. Conclusion

In this paper, we investigated the impact of the non-uniform distribution of scatterers along with the non-omnidirectional APPs on the PSD for a 2D-WB/UWB MISO channel. The PSD is the result of the Fourier analysis of the CCF in a stationary case. It was observed that the PSD deviates from the U-shaped function, i.e., Clarke/Jake model. This deviation depends on the AAS, the employed antennas, and the direction of the MS speed. The results also prove that the range of frequencies over which the channel operates as well as the channel bandwidth have a great impact on the behavior of these characteristics.

References

[1] A.M. Piştea, H. Rad, T. Paladeand A. Moldovan, Cross correlation function for wideband MIMO channels: derivation and analysis. Proceedings of the 6th International Wireless Communications and Mobile Computing Conference, pp. 819-823, July 2010,

[2] R. B. Ertel, P. Cardieri, K.W. Sowerby, T. S. Rappaport, and J. H. Reed, Overview of spatial channel models for antenna array communication systems. IEEE Pers. Commun., vol. 5, pp. 10–22, February 1998.

[3] K. Yu. Multiple-Input Multiple-Output Radio Propagation Channels: Characteristics and Models. Doctoral thesis, Signals, Sensors and Systems, Royal Institute of Technology (KTH), 2005.

[4] Y. Ma and M. Pätzold, Wideband two-ring MIMO channel models for mobile-to-mobile communications. Proc. 10th International Symposium on Wireless Personal Multimedia Communications, WPMC 2007. Jaipur, India, pp. 380–384, Dec. 2007.

[5] M. Pätzold and B. O. Hogstad, A wideband MIMO channel model derived from the geometric elliptical scattering model. Processing of 3rd International Symposium on Wireless Communication System, pp. 138–143, Sept. 2006.

[6] C.-C. Chong, C.-M. Tan, D. I. Laurenson, S. McLaughlin, M. A. Beach, and A. R. Nix. A new statistical wideband spatio-temporal channel model for 5-GHz band WLANsystems. IEEE J. Select Areas Commun., vol. 21, pp. 139–150, Feb. 2003.

[7] A. Balanis. Antenna theory: analysis and design. John Wiley & Sons, 2 edition, 1996.

[8] H.S. Radand S. Gazor, The Impact of Non-Isotropic Scattering and Directional Antennas on MIMO Multicarrier Mobile Communication Channels. IEEE Transactions on Communications vol. 56, no. 4, pp. 642-652, Apr. 2008.

[9] Q. Spencer, M. Rice and M. Jensen. A statistical model for the angle of arrival in indoor multipath Propagation, IEEE Vehicular Technology Conference, pp. 1415-1419, 1997.

[10] A. Abdi, J. Barger, and M. Kaveh, A parametric model for the distribution of the angle of arrival and the associated correlation function and power spectrum at the mobile station. IEEE Trans. Veh. Technol., vol. 51, no. 1, pp. 425–434, May 2002.

[11] K. Haneda and J. Takada, An application of SAGE algorithm for UWB propagation channel estimation. Proc. IEEE Conf. Ultra Wideband Systems and Technologies 2003 (UWBST2003), Reston, VA, USA, pp. 483-487, Nov. 2003.

[12] G. D. Durgin, Theory of stochastic local area channel modeling for wireless communications. Ph.D. dissertation, Virginia Tech, Blacksburg, VA, Dec. 2000.

[13] J. D. Parson and A. M. D. Turkmani, Characterisation of mobile radio signals: Base station crosscorrelation. IEE Proceedings I. Communications, Speech and Vision, 138(6), pp.557–565, December 1991.

[14] J. D. Parson and A. M. D. Turkmani, Characterisation of mobile radio signals: Model description. IEE Proceedings I, Communications, Speech and Vision, vol. 138(6). pp. 549–556, Dec. 1991.